

Geotechnical risks in natural recreational areas: a case study of potential geotechnical hazards in a Western Australian national park and other parts of the world

G Owusu-Bempah *Rio Tinto, Australia*

Abstract

In recent years, numerous global geotechnical-related fatalities have occurred globally. These fatalities are not solely confined to the mining industry, as many tourist destinations have also experienced catastrophic events from rockfalls. While tourists enjoy their beautiful surroundings they may be unaware of the rising geotechnical risks in these locations, which may result in loss of life if not effectively addressed. Many of these holiday destinations have unfavourable ground conditions which require careful consideration, including monitoring inspections, restrictions and adequate controls. Hiking corridors, beachfront scarps and national park walkways are just a few locations known for high-risk rockfall issues, slope failures or exposed outcrops that pose a potential hazard. Unfortunately, many of these locations require access restrictions due to unstable geotechnical conditions. As the geotechnical risks in tourist locations continue to increase, the geotechnical community, local governments and the tourism industry must work together to effectively manage these hazards. Tourism regulators and local governments must engage geotechnical engineers to inspect and analyse exposed geotechnical risks and provide workable remediation controls to reduce tourist exposure to rockfall. This paper presents several case studies in the Pilbara region of Western Australia and other parts of the world to highlight the geotechnical hazards and subsequent rockfalls that tourists may become unwittingly exposed or need to be aware of. It aims to raise awareness for additional control measures such as exclusion zones through rockfall simulation that can be adopted to mitigate some of the life-threatening rockfall issues. The paper also highlights the opinions of prospective tourists on rockfall perception using sample photographs of some tourist locations based on operators' promotional material and how these perceptions can be geotechnically interpreted remotely to highlight the risks of using Google Earth 3D and satellite imagery.

Keywords: *natural hazards, tourism industry, local governments, geotechnical risk, rockfall fatalities, adverse ground condition, rockfall simulation, exclusion zones*

1 Introduction

The Pilbara region in Western Australia (WA) is renowned for its stunning landscapes featuring caves and gorges that have been eroded and weathered, with boulders that are almost detachable due to harsh weather conditions. These attractions are commonplace in surrounding tourist areas. For many years these locations have experienced increased tourism activity without any formal notification to the general public of the potential risk posed by detachable rocks in dangerous areas such as steep slopes, access tracks, walking tracks and scarps. Some of these areas are located within or close to mining tenements where workers engage in physical exercise before and after their shifts, such as on a walking track within one of the mine tenements in the Pilbara which is approximately 2 km long and in a valley of severely weathered and hydrated hardpan. However, the risks of rockfall there are adequately managed by mining companies by bringing the risk to as low as reasonably practicable (ALARP) or near-zero probability; something the relevant local government could adopt in tourist areas. The track is in a valley with moderately to highly steep slopes, just as in other parts of the world where rockfall hazards are evident in rocky locations. The track is characterised by large, detached rocks of various sizes on the western sides of the scarps, some of which are up to 8 m long and about 3 m to 4 m in diameter. In some locations the track has been diverted because of rolled rocks

2 Perception of prospective tourists and tourism operators in some rocky tourist locations

[illegible]

664

3 Remote assessments of rockfall hazards in tourist locations using Google Earth 3D Studio and satellite imagery

In this paper, both Google Earth Studio, a browser-based animated applications tool for Google Earth 3D, and satellite imagery were used to provide clear photogrammetry images with fine details for describing geotechnical risks in remote holiday locations. The application allows remote assessment to describe geological characteristics so as to understand stability conditions. Generally, most of the populous tourist destinations are found on Google Earth 3D. Google Earth Studio has a camera functionality that can focus on a preferred angle and direction for capturing a remote photograph from a Google 3D satellite image. In this paper, some of the pictures taken with a Google Studio camera have been presented in Section 4 and subsequent sections. In the locations where the Google Earth Studio 3D image is blurry due to reduced resolution from zooming, GPS-registered photographs of the area taken by individuals on Google Earth were utilised as sources for photographs to describe the geotechnical risk and rock features. The images enable a closer view to identify the risk of rockfalls and plausible structural characteristics culpable for inducing instabilities. Also, a near-accurate persistence of the structures can be measured to support part of the remote assessment. Figure 2 shows Google Earth Studio camera photographs of Yosemite National Park igneous rocks in the USA, with cracks and overhang, and slope instability in limestone in Naviago Beach, Zakynthos Island, Greece.

Saroglou et al. (2019) published and used an unmanned aerial vehicle (UAV) for capturing and mapping the Corinth Canal in Greece to determine slope failure instability that closed the canal. The point cloud data from the UAV was used to create a 3D reality model of the slope for stability analysis, and a similar concept was used to model the slope for rockfall analysis. Drone photogrammetry and point cloud data methodology for gathering remote data have become standards for collecting defect characteristics and properties that influence slope instability. In addition to using Google Earth, UAV point cloud survey data in combination with field reconnaissance techniques were employed for assessing the rockfall risk on the walking track in a recreational location in the middle of the Pilbara (previously described in this paper). The point cloud data from the UAV was used for creating a 3D slope geometry for rockfall simulation to determine rockfall runout distances and energy generated by the detached rocks. This could encourage local governments and tourism operators to adopt drone technology to assist in conducting remote geotechnical assessments of national parks in collaboration with geotechnical engineers so as to adopt a remedial control to save the lives of holidaymakers in rocky tourist locations.

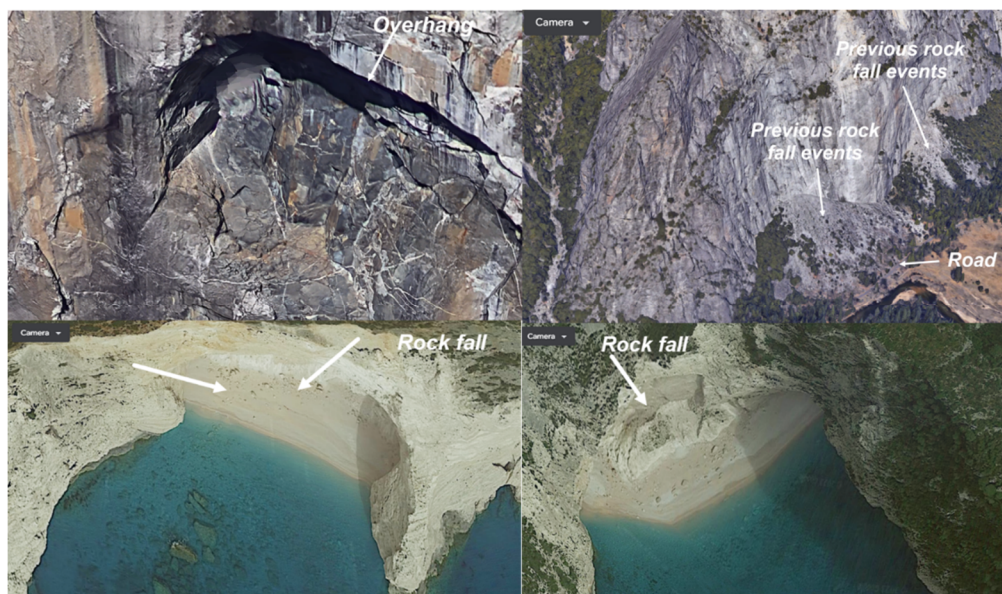


Figure 2 Google Earth Studio camera image of Yosemite National Park igneous rocks in USA showing joint structural defects and overhang on the top photograph and slope failure and rockfall in limestone in Naviago Beach in Zakynthos Island, Greece, bottom photograph

4 A geotechnical perspective of some of the remote tourist locations

4.1 Karijini National Park

Karijini is a well-known tourist destination in the Pilbara region frequented by locals, mining workers and visitors seeking picturesque scenery, adventure and a place to unwind. However, it is essential to note that some areas within the park have a high-risk of rockfall, which poses a severe threat to visitors. This risk is due to the morphology of the exposed rocks, which are characterised by tension cracks, hydration and ruggedness exacerbated by the region's extreme weather conditions. In 2015 a 19-year-old man was killed when the 7 m-high ledge he was sitting on collapsed. Moreover, the growth of vegetation roots in these cracks also exacerbates the risk of rockfalls. Figure 3 shows a tourist walkway under overhanging rock with visible multiple joints and tension cracks; a leading cause of rockfall instabilities. The bedded rock with jointing is part of a weathered rock within the Hamersley Group in the Pilbara. Details of the Hamersley Group stratigraphic geology have been defined in the streamlining geotechnical slope reconciliation for the open pit in Brockman 2 in the Pilbara paper (Owusu-Bempah 2020). Even though the authorities at Karijini National Park have displayed rockfall signs at certain locations, it does not indicate areas of severe rockfall or exclusion zones. Often the rockfall areas are the access points to the next location within the park.



Figure 3 Google Earth-registered photograph of the rockfall risk over a walkway grating with exposed bedding and joints in Karijini National Park in the Pilbara, Western Australia

4.2 El Capitan rockfall in Yosemite National Park, USA

El Capitan is in Yosemite National Park, USA. In February 2023 a huge rock fell from the cliff side, landing close to a tourist. This event was recorded by someone in the vicinity at the time. However, that was not the only recorded rockfall incident at El Capitan. In 2017 a tourist died after a rockfall event. Similarly, in 2022, two people died after a rockfall landed on them. Besides recent rockfall events and subsequent fatalities, several other fatalities have been recorded in this populous tourist destination owing to rockfalls from the scarp or mountaineering. Over 38 deaths have been recorded in total, including those rockfall related. This has yet failed to result in stringent control measures from local authorities to protect tourists from such rockfall risks.

The geology of El Capitan is composed predominantly of pale, coarse-grained granite approximately 100 Ma old. The western portions of Yosemite Valley are mainly composed of a separate granitic body called Taft granite. Both kinds of granite had been documented as having dark-vein dolerite intrusion, which is prominent in the area known as North America Wall, having the greatest influence on rockfall risk in the area. Although granitic rock is unbroken on a small-scale, on a larger scale the rock is broken by joints which are planar cracks commonly found as sets of parallel fractures in the rock (Huber 1987). The joint structures are plausible for present rockfall events and the risk of overhangs could result in future potential rockfalls. Figure 4 shows a Google Earth satellite image of the Yosemite granite with multiple intersecting joints.

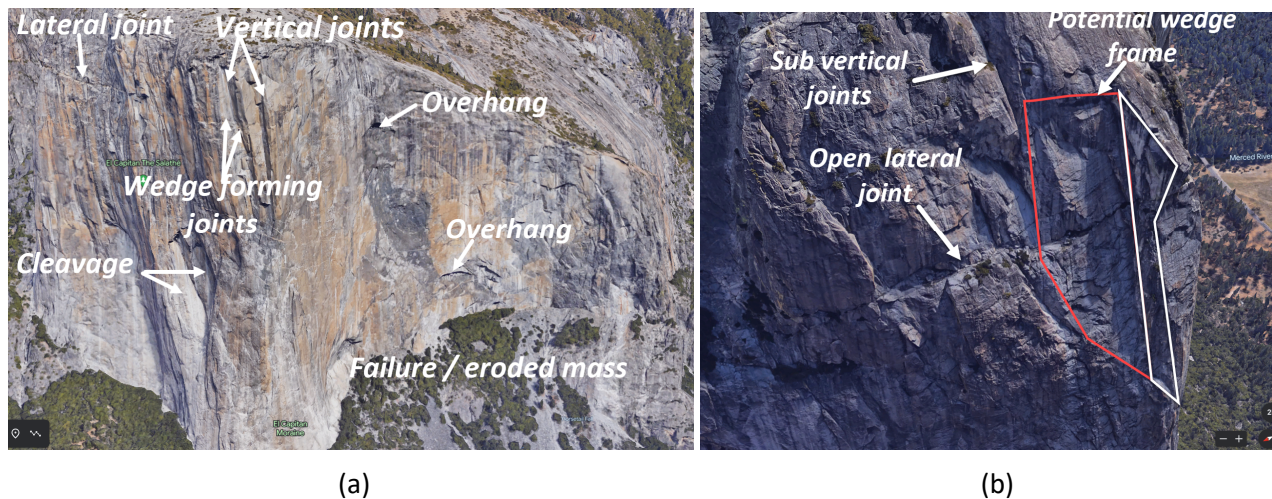


Figure 4 Google Earth Studio satellite image of Yosemite National Park igneous rock. (a) Intersecting parallel joint discontinuities and overhang; (b) Camera image of the rock at different angle showing the potential wedge frame

4.3 Navagio Beach, or Shipwreck Beach, on Zakynthos Island, Greece

Zante beach in Greece is a well-known location that experienced an unfortunate rockfall event when seven tourists were injured due to tonnes of rock falling after an earthquake. Rockfall events are generally common there and often associated with other controlling factors at the beach because of the geology, climatic conditions and high vertical slope face. From the photographs in Figure 5, it appears the area is predominantly comprised of weathered limestone with multiple discontinuities. The exposed face of the rocks shows converging sub-vertical joint sets forming various block sizes for potential wedge instability. Erosion, caused by ocean wave currents which scour the rock face and form cavities, brings the sub-vertical joints into tension and results in the potential collapse or fall of ground. The unsupported roof of the cavities subsequently cause potential rockfalls. Frequently these pockets of eroded cavities are popular tourist attractions, which exposes visitors to rockfall impact zones.

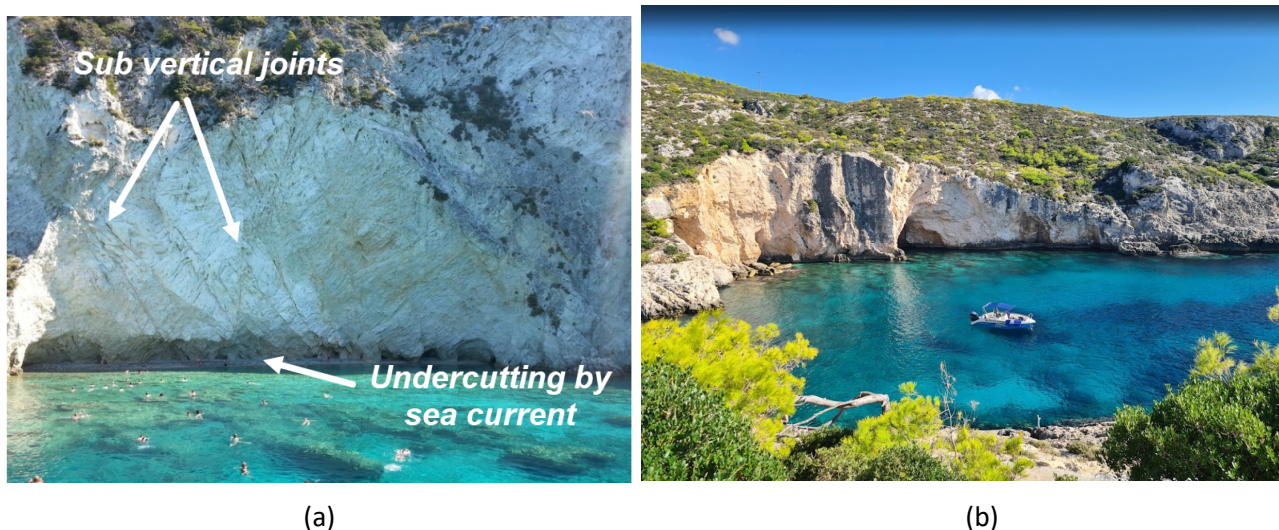


Figure 5 Google Earth-registered photographs of a beautiful clear blue ocean with limestone rock at Zakynthos Island, Greece: (a) Sub-vertical and intersecting joints with potential for a wedge-forming block; (b) Distance photograph of the landscape and eroded cavities

4.4 Furnas Lake, Minas Gerais, Brazil

Lake Furans in Minas Gerais, Brazil, serves as a hydroelectric dam. The area around the dam has many attractive canyons and waterfalls that attract tourists. Unfortunately, tragedy struck early in 2022 when a rockfall event killed 10 tourists on a speed boat cruising around the exposed face of the canyon rock. The video from the scene indicated a toppling failure mechanism. The head of Brazil's geological services had 'warned that the location has been subjected to centuries of erosion, leaving it vulnerable to rain, heat, and cold'. Ongoing natural erosion is likely to cause more rockfalls during the rainy months of December and January' (CBS News 2022). However, the warnings from authorities seemed not to have been heard by adventure seekers and local operators, or at least did not prevent tourists wanting to get closer to the rock face. A closer examination of Google Earth-registered photographs reveals that the cliff face is in an area with adverse geotechnical conditions characterised by both horizontal and vertical joint sets, as shown in Figure 6. Some of the vertical joints are nearly 90° and have long trace lengths, making them particularly susceptible for toppling rockfall and sliding failure mechanisms during inclement weather conditions; thereby rendering the area geotechnically unstable. It is crucial for tourists to exercise caution when visiting these areas and to pay attention to any warnings from local authorities.

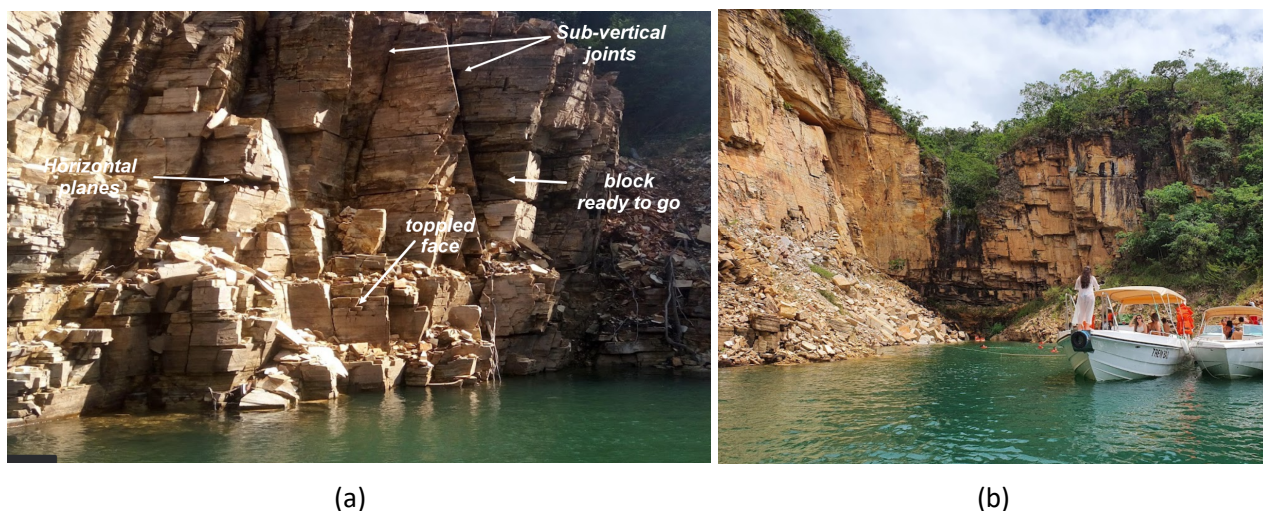


Figure 6 Google Earth-registered photograph of Furnas Lake, Minas Gerais, Brazil, showing (a) Sub-vertical joints and horizontal plane openings susceptible to wedge and toppling failures; (b) A far-view photograph of failed material and overhang rocks

5 A case study rockfall simulation of the walking leisure track in Western Australia

5.1 A walking track in the Pilbara

The walking track in a valley behind a mining village (see Section 1) spans nearly 2 km and is confined by approximately 40 m-high slopes on both sides, with facades. The physical geology of the area generally consists of huge crumbled hydrated rock from the facade, with rockfall hazards typically associated with the western side of the cliff. However, certain areas of the track have been impacted by rocks, making it more precarious in those locations. In places where rocks have rolled onto or blocked parts of the track, the track has been diverted to manage the increased risk; highlighting the importance of managing risks in tourist locations with prevalent rockfall hazards. Measures must be taken to mitigate the risk of rockfalls for personnel who use the track regularly. Figure 7 shows the walking track and locations of the detached rocks, including rocks used in rockfall simulations.

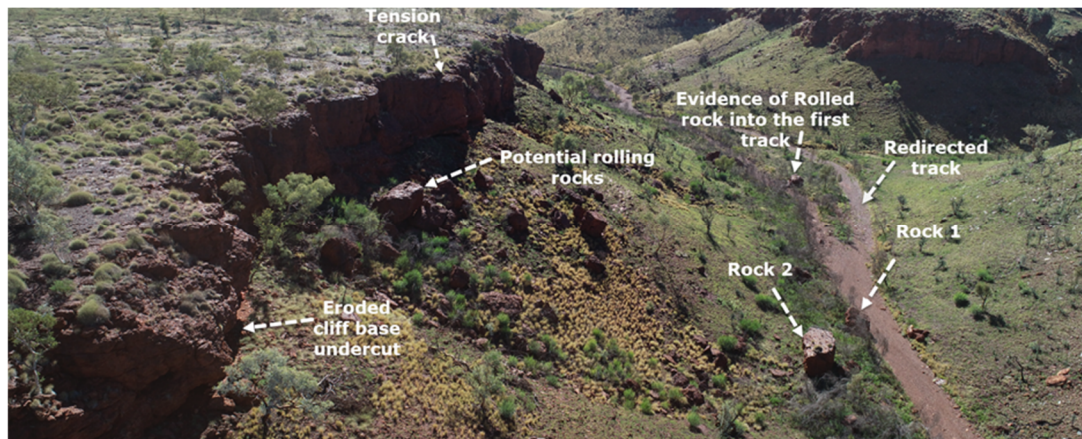


Figure 7 An aerial photograph of the slope and the walking track showing loose rocks from the facade used in rockfall simulation, behind a mining village in the Pilbara, Western Australia

Rockfall analyses were undertaken on this walking leisure track to assess rockfall hazards and establish a safe zone to prevent rockfalls from impacting on people. The slope profiles in the models were obtained from an UAV, and point cloud data were generated and processed in Maptek Vulcan, as shown in Figure 8a. Back-analysis on lump mass and rigid body methods was performed in Rocscience, Rockfall2.f18. The energy and end point locations were determined by simulating the trajectory of the two rocks close to the walking track.

The slopes were analysed in two topographical cross-sections for rocks 1 and 2, as shown in Figure 8b. The analyses were performed mainly on the west slope of the valley, where Pilbara hydrated rocks are seen to have detached from the cliff at 574 RL and landed at 535 RL. The slope profiles from the detachment zones have a steeper slope angle and transitioned into an average slope gradient with a few centimetres-high vegetation cover. The vegetation cover on the slope was conservatively modelled at 10 cm-high in rigid body analysis.

Table 1 summarises the physical dimensions of the two analysed rocks (seeder) with other rocks within the rockfall zone. Results from the back-analyses are detailed in Section 5.2 for rigid body and lump mass simulations. The average kinetic energies determined indicate that the intensity of the rocks from the sources to the resting position do not dissipate energy and represent the forces rolling rocks could have on the impact. The estimated energy could be useful for selecting a potential rockfall stabilisation mesh or rockfall fence, creating an exclusion zone or rock scaling to save lives.

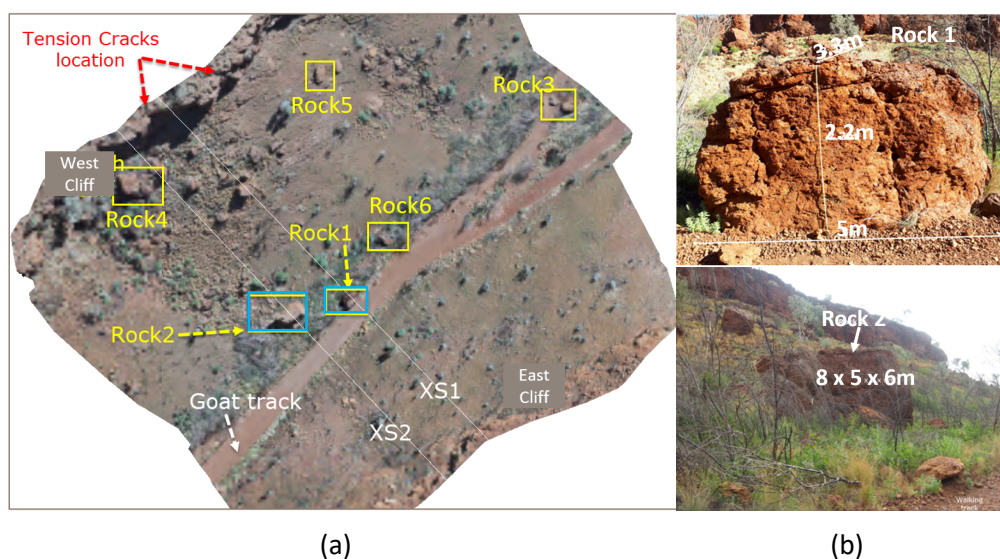


Figure 8 (a) Two topographical cross-sections (XS1 and XS2) of Rocks 1 and 2 used in a rockfall simulation; (b) Photographs of actual rocks and resting positions

Table 1 Dimensions of the seeder input material properties of the Pilbara hydrate rock used

Seeder	Rock type	Length (m)	Width (m)	Height (m)	Volume (m ³)	Density (kg/m ³)	Mass (kg)
Rock 1	Hydrated rock (HYD)	5.0	3.3	2.2	36.3	2,700	98,010
Rock 2		8.0	5.0	6.0	240.0	2,700	648,000
Rock 3		4.5	3.3	2.0	29.7	2,700	80,190
Rock 4		6.4	5.0	6.0	192.0	2,700	518,400
Rock 5		3.6	3.3	1.0	11.9	2,700	32,076
Rock 6		4.0	3.2	2.3	29.4	2,700	79,488

5.2 Back-analysis simulation of Rocks 1 and 2

The end point locations of rocks were accurately predicted and trajectory analyses of actual rocks were back-analysed retrospectively. The average friction angles were determined along the slope profiles using the changes in gradients on the slope along the trajectory of the rocks path. The average friction angle of 75° was used, equivalent to the slope gradient of 81 and 70° as determined by the geometry of cross-section 1 within the hydrated (HYD) material. For cross-section 2, a friction angle of 73°, equivalent to the slope gradient within the HYD zone, was used. The slope defined as rill material in the model ranged from 25 to 33° and approached a near-flat slope profile close to the walking track. An average frictional angle of 26° for cross-section 1 and 29° for cross-section 2 accounted for resistance of the rill material and vegetation cover. Analysis was simulated using representative shapes of the rocks in each cross-section as seen in the field. A squared, smooth shape was used for Rock 1, while a rectangular shape was simulated for Rock 2. A slight level of conservatism was introduced in shape modelling for Rock 2 since it was not perfectly rectangular as modelled. In total four analyses were simulated: two in rigid body and two in lump mass. In all, 100 rocks were simulated, and a summary of back-analysed rock properties was tabulated.

It was found that the rolling rocks were sensitive to normal and tangential restitution, including horizontal velocities. The typical horizontal velocities from the analyses ranged from 0.24 to 1.3 m/s, as shown in Table 2. The coefficient of normal restitution and tangential restitution values were obtained, representing the back-analysis results of both rigid body and lump mass simulations as shown in Tables 2 and 3, respectively.

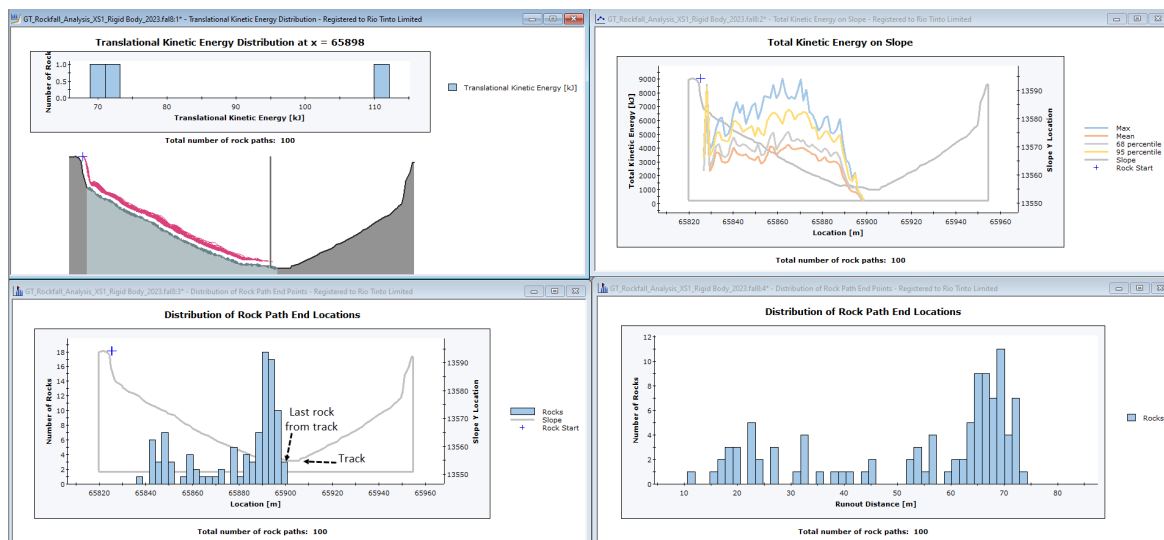
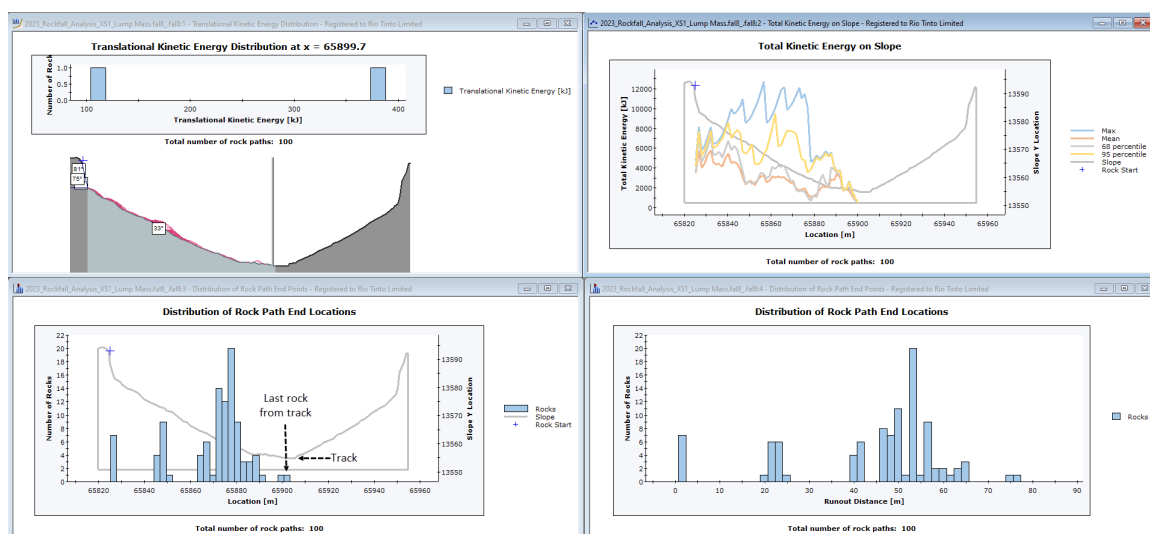
Table 2 Rigid body simulation back-analysis results for cross-sections 1 and 2

Analysis method	Section	Material	Normal restitution (Rn)	Tangential restitution (Rt)	Dynamic friction	Rolling friction	Vegetation cover (m)	Drag coeff	Horizontal velocity (m/s)
Rigid body	1	Hydrated rock (HYD)	0.33	0.87	0.47	0.21	0	0	1.3
		Slope mat (rill)	0.32	0.88	0.5	0.3	0.1	500	
	2	Hydrated rock (HYD)	0.34	0.88	0.5	0.16	0	0	1.2
		Slope mat (rill)	0.35	0.87	0.5	0.36	0.1	500	

Table 3 Lump mass simulation back-analysis results for cross-sections 1 and 2

Analysis method	Section	Material	Normal restitution (Rn)	Tangential restitution (Rt)	Friction angle (°)	Rotational velocity friction	Horizontal velocity (m/s)
Lump mass	1	Hydrated rock (HYD)	0.34	0.86	75	0.5	0.24
		Slope mat (rill)	0.37	0.88	26		
	2	Hydrated rock (HYD)	0.34	0.88	73	4	1.2
		Slope mat (rill)	0.33	0.87	29		

The results of the rockfall analyses of the four simulations have been presented in Figures 9 to 12.

**Figure 9 Chart distribution showing rigid body back-analysis results of estimated energies of the endpoints and a runout distance of cross-section 1 for Rock 1****Figure 10 Chart distribution showing lump mass back-analysis results of estimated energies of the endpoints and a runout distance of cross-section 1 for Rock 1**

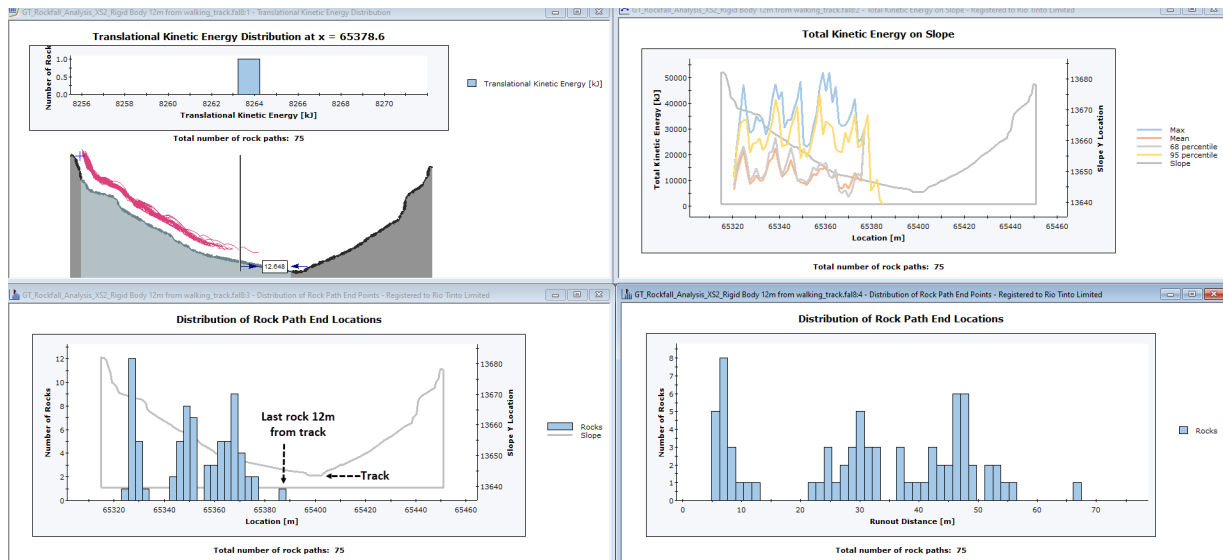


Figure 11 Chart distribution showing rigid body back-analysis results of estimated energies of the endpoints and a runout distance of cross-section 2 for Rock 2

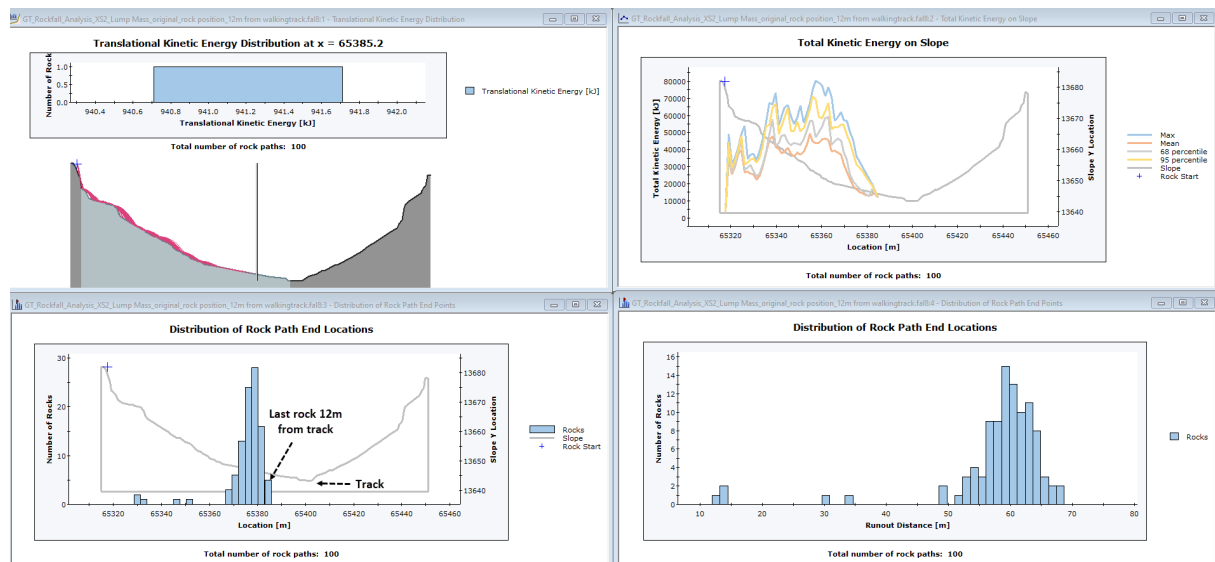


Figure 12 Chart distribution showing lump mass back-analysis results of estimated energies of the endpoints and a runout distance of cross-section 2 for Rock 2

5.3 Rockfall simulation results

The simulation results for cross-section 1 demonstrate that the last rock came to rest near the edge of the walking track, consistent with field observations. The rigid body simulation indicates that the last rock for this section came to rest at approximately 74 m, representing the runout distance and end point location from the cliff. For the lump mass simulation of Rock 1, a runout distance of 76 m was obtained. The difference in runout distances between the rigid body and lump mass simulations is approximately 2 m. The total kinetic energy obtained at the resting position from Rock 1 at the edge of the walking track was 201.4 kJ for the rigid body simulation and 499.9 kJ for the lump mass simulation.

Regarding cross-section 2, the simulation results indicate that the last rock rested at approximately 12 m from the walking track, consistent with field observations for Rock 2. For the rigid body simulation, the end point of Rock 2 came to rest at approximately 67 m, representing the runout distance. The lump mass simulation resulted in a runout distance of 68 m for Rock 2. The difference in runout distances between the

rigid body and lump mass simulations is approximately 1 m. The total kinetic energy of the rocks at the resting position was 10682.7 kJ for the rigid body simulation and 12792 kJ for the lump mass simulation.

The difference in runout distance between the two methods is only 2 m and 1 m, respectively, for both cross-sections of the rocks. Therefore, either ridge body or lump mass simulation methods could be employed to determine a runout distance or endpoints of the rocks in rockfall analysis for the cases discussed in Section 4.

Overall, the simulations for both cross-sections indicate that energy from falling rocks is not dissipated between the starting and end point, making any area between the starting point on the facade and the last rocks unsafe. Thus this area could be designated as a high-risk/exclusion zone, with the area beyond Rock 1 considered safer for people. It is also noted that the impact within the transition zone could be severe. Figure 13 illustrates the rockfall simulation trajectory indicating a potential designated a high-risk/exclusion zone and a safer zone.

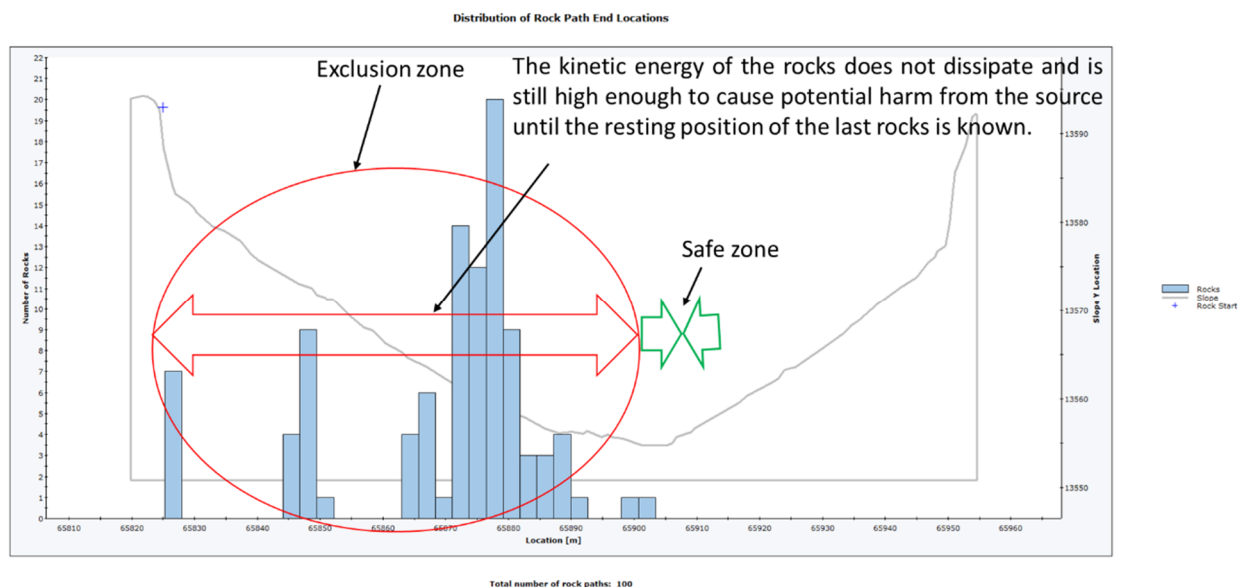


Figure 13 Distribution of rock path end point locations showing a rockfall intensity no-go zone as an exclusion zone, and a safe zone beyond the last rock on the track

6 Conclusion

The survey indicates that tourists need to be made aware of the geotechnical risks present at these tourist locations. While some tourist locations have rockfall signages displayed, more can be done by local governments and tourism operators, with the assistance of geotechnical engineers, to identify and analyse such risks to reduce the consequence of rockfall risk to ALARP.

Geotechnical engineers could undertake a remote geotechnical assessment in numerous tourist locations by utilising tools such as Google Earth 3D GPS-registered photographs and Google Earth Studio with satellite imagery, including the use of UAV tools. By analysing the risk of rockfall, local governments and tourism operators can take necessary steps to ensure the safety of tourists.

Having successfully predicted the endpoints of the rocks using rockfall analysis in this paper means that the methods employed are replicable in the popular tourist locations of the cases discussed in Section 4 to demarcate a safer zone so as to manage tourist exposure to rockfall.

Based on the results of the rockfall simulation, the endpoints align well for two rocks near the walking track. Additionally, the back-analysis results may be applicable for similar large rocks in similar conditions. The average kinetic energy of rocks dissipates when in their resting positions, while the area between their start and end locations must be considered exclusion zones. Recently Ge et al. (2021) found out that the less energy the rolling rock consumes in the process of moving on the slope, the more total kinetic energy is left

while rockfall reaches the bottom of the slope. This means the rocks could have enough kinetic energy for a severe consequence even where the slope gradients are seen as shallow in the resting locations.

Acknowledgement

The author acknowledges: Google and its staff for providing the account and installation files of Google Earth Studio; people (potential tourists) who participated in the photographsurvey; Rio Tinto for using the Rocscience application for the rockfall simulations; and Benjamin Luff for providing different perspective photographs of Karijini National Park.

References

- CBS News 2022, 'Dramatic video captures cliff collapsing on tourist boats, killing 10 in Brazil', CBS News, viewed 10 January 2022, <https://www.cbsnews.com/news/brazil-cliff-collapse-10-killed-video>
- Ge, Y, He, XR, Yuan, XQ, Pu, XY, Meng, LD, Wang, HK & Huang, YY 2021, 'Analysis of rockfall hazards stopping position and energy dissipation based on orthogonal experiment', *E3S Web of Conferences* 261, <https://doi.org/10.1051/e3sconf/202126101004>
- Huber, NK 1987, *The Geologic Story of Yosemite National Park*, Bulletin 1595, US Geological Survey, Reston.
- Owusu-Bempah, G 2020, 'Streamlining geotechnical slope reconciliation for open pits, a slope optimization and recommendation approach at Brockman 2 Operations in the Pilbara Region in Australia', *Proceedings of Sixth UMaT Biennial International Mining and Mineral Conference*, Tarkwa, pp. 33-42.
- Saroglou, C, Bar, N, Manousakis, J & Zekkos, D 2019, 'Analysis of slope instabilities in the Corinth Canal using UAV-enabled mapping' *Second International Conference on Natural Hazards and Infrastructure*, Chania.